Modulating the properties of monolayer C_2N: A promising metal-free photocatalyst for water splitting*

Song Yu(俞松), Yong-Chao Rao(饶勇超), and Xiang-Mei Duan(段香梅)†

Department of Physics, Faculty of Science, Ningbo University, Ningbo 315211, *China*

(Received 10 April 2017; revised manuscript received 8 May 2017; published online 10 July 2017)

Photocatalytic water splitting has gained increasing attention, since it utilizes renewable resources, such as water and solar energy, to produce hydrogen. Using the first-principles density functional theory, we investigate the properties of the single layer C_2N which was successfully synthesized. We reveal that monolayer C_2N has a substantial direct band gap of 2.45 eV. To regulate its band gap, four different nonmetal elements (B, O, P, and S) on the cation and anion sites are considered. Among them, B-doped N site is the most effective one, with the lowest formation energy and a band gap of 2.01 eV. P-doped N site is the next, with a band gap of 2.08 eV, though its formation energy is higher. The band alignments with respect to the water redox levels show that, for these two dopings, the thermodynamic criterion for the overall water splitting is satisfied. We therefore predict that B- or P-doped C_2N, with an appropriate band gap and an optimal band-edge position, would be a promising photocatalyst for visible-light water splitting.

Keywords: C_2N, metal-free photocatalyst, water splitting, doping, first-principle calculation

PACS: 73.20.At, 71.15.Mb, 71.20.Nr **DOI:** 10.1088/1674-1056/26/8/087301

1. Introduction

With increasing serious energy and environment problems, searching for sustainable clean energy sources has become an important research topic. Owing to its high energy capacity and environmental friendliness, hydrogen has been identified as one of the best possible alternative energy carriers.[1–4] However, the main challenges in developing hydrogen energy are its generation and storage. Hydrogen generation through photocatalytic water splitting using solar energy is a perfect method that does not evolve any harmful by products.[5,6]

Stimulated by the fact that Fujishima reported photocatalytic 7litting of water on n-type TiO_2 electrodes in 1972,[7] the search for suitable semiconductors as photocatalysts for water splitting to produce hydrogen has been considered as one of the noble missions of material science. Unfortunately, despite intense efforts during the past two decades, most of photocatalysts, like metal oxides, sulfides, and nitrides with d_0 or d_{10} transition metal cations,[8–14] still face some challenging issues, such as the inability to utilize visible light, low quantum efficiency, poor stability, and high cost.[15,16] So researching and developing the novel materials with high efficiency and stable photocatalytic property is need to ongoing.[17] Other than these conventional materials, polymeric semiconductor materials like graphitic carbon nitrides are also shown great potential as photocatalyst. Wang *et al.*[18] have reported the melem-based graphitic carbon nitrides (g-C_3N_4) as a metal-free photocatalyst for visible-light driven water splitting. However, this material shows very poor quantum yield, which is attributed to the high recombination rate of the photogenerated electron–hole pairs. To modulate its properties, many attempts have been made, namely, doping, metal decoration, introducing porosity, making graphene/g-C_3N_4 composites,[19–22] etc. It has been shown that the carrier mobilities of g-C_3N_4 nanotubes are higher in comparison with the two-dimensional (2D) sheets, and functionalization of these tubes with metals like Pt and Pd could further enhance its photocatalytic activity.[23] The g-C_3N_4/MoS_2 nanocomposites have also exhibited better photocatalytic activity.[24] C_2N is another polymeric carbon nitride apart from the g-C_3N_4, recently, a layered 2D network structure of C_2N has been successfully synthesized under ultrahigh vacuum conditions. An FET based on layered C_2N with a high on/off ratio of 10^7 was fabricated and it possesses an optical band gap of 1.96 eV.[25] These findings make C_2N sheet a very promising candidate for future applications in nanoelectronics and optoelectronics. The further studies on C_2N is quite necessary.

In the present study, using first principles calculations, we explore the properties of a single layered C_2N and the effect of substitutional doping with different nonmetal elements, boron, oxygen, phosphorus, and sulfur. Analogous studies on g-C_3N_4 are also being carried out to compare the computational results with the existing experimental results. We find that the monolayer C_2N has a direct band gap of 2.45 eV at the Γ points. The doped C_2N remains its direct bandgap characteristic. The band alignments of pure C_2N and doped C_2N with respect to the water redox levels show that they are the satisfied overall requirements for the water splitting. Comparatively, the doped C_2N

*Project supported by the National Natural Science Foundation of China (Grant No. 11574167).

†Corresponding author. E-mail: duanxiangmei@nbu.edu.cn

© 2017 Chinese Physical Society and IOP Publishing Ltd

has better visible-light adsorption, and among the dopants we considered, boron- and phosphorus-doped C_2N could be good metal-free photocatalyst candidates.

2. Calculation methods

All our density functional theory (DFT) calculations are carried out using the projector augmented wave (PAW)[26,27] potentials as implemented in the first principles-based Vienna *ab initio* Simulation Package (VASP).[28,29] Plane-wave basis sets with a kinetic energy cutoff of 520 eV have been used. The exchange–correlation energy density functionals are treated through the generalized gradient approximation (GGA) of Perdew–Burke–Ernzerhof (PBE).[30] The convergence criteria is set to be 10^{-5} eV for the electronic self-consistent field iterations. The atomic positions are optimized until the maximum Hellmann–Feynman force on each atom is less than 0.001 eV/Å. The first Brillouin zone is sampled with Monkhorst–Pack grid of $5 \times 5 \times 1$ for structure optimization and $9 \times 9 \times 1$ for static calculation. Since PBE functional is well known to underestimate the band gap, we also use the more accurate hybrid functional HSE06[31] to calculate band structure. All the initial geometries and the reported figures are generated using the VESTA.[32]

The formation energy, E_f, describes the relative difficulty for different ions to be incorporated into the host lattice and is a widely accepted gauge of energetic stability. The formation energy of a substitutional dopant on nitrogen site, for instance, is defined by

$$E_f = E_{doped} - E_{clean} - \mu_{dopant} + \mu_N, \quad (1)$$

where E_{doped} is the total energy of the system containing the dopant, E_{clean} is the total energy of the pure C_2N sheet, μ_{dopant}, and μ_N are the chemical potential of the dopant atom and N atom. The greater the formation, the more difficult the doping.

3. Results and discussion

We first study the geometric properties of monolayer C_2N. The atomistic ball-stick models of monolayer C_2N with a unit cell is illustrated in Fig. 1(a), where there are 12 C atoms and 6 N atoms and uniform holes. This planar structure is fully relaxed according to the force and stress calculated by DFT within the PBE functional. The equivalent lattice parameter of monolayer C_2N is found to be 8.33 Å(the experimental value is 8.30 Å,[25]) generating the in-plane covalent bond lengths as C–C of 1.43 Å and C–N of 1.34 Å. A direct band gap of 1.66 eV at the Γ points is observed with PBE, and the value is 2.45 eV via the HSE06, which is consistent with previous study, the experimental band gap is 1.96 eV.[25]

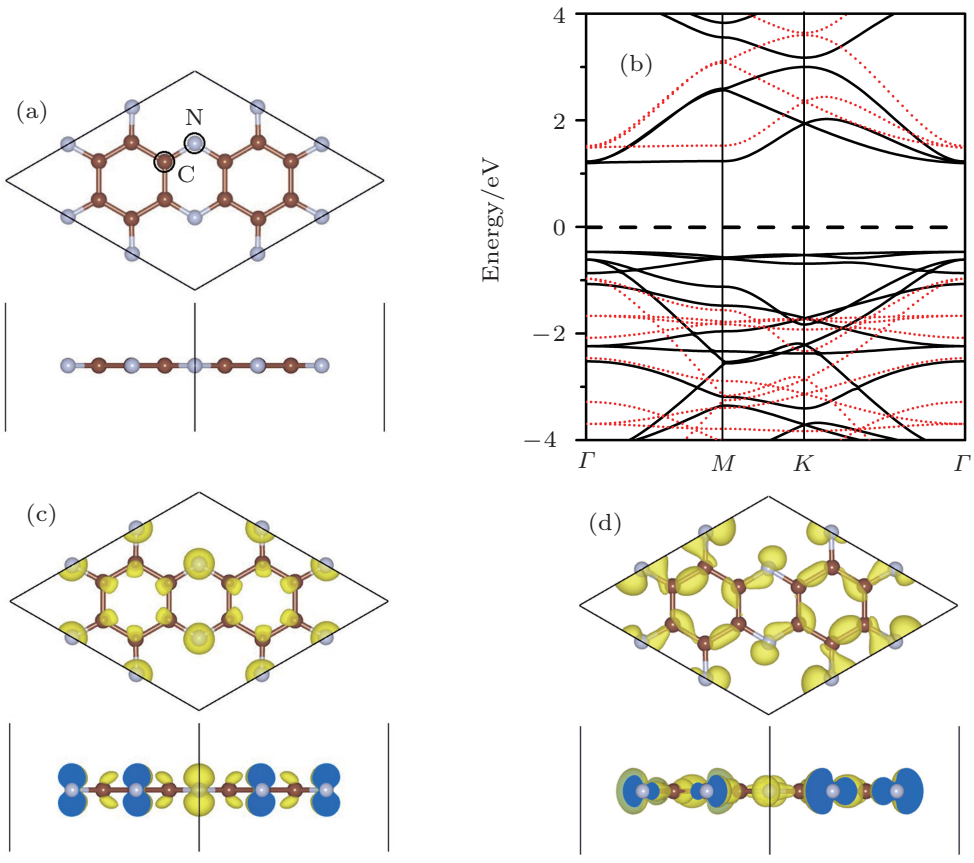


Fig. 1. (color online) (a) Top view and side view of the geometric structure of monolayer C_2N. The brown and grey spheres represent C and N atoms, respectively. (b) Band structures of monolayer C_2N calculated by PBE (black solid lines) and HSE06 (red dashed lines). Panels (c) and (d) are the charge density corresponding to CBM and VBM, respectively. The isovalue is set to be 0.03 e Å^{-3}.

Figure 1(b) shows the band dispersion plots of C_2N with the PBE and HSE06 functionals. It can be seen that both the valence maximum (VBM) and conduction band minimum (CBM) are well dispersed and there is no localized states, which can avoid the recombination of the photogenerated electron–hole pairs. Unlikely, g$-C_3N_4$ has many localized band edges close to the band edges, which would be the reason for its low quantum efficiency.[23,33] More specifically, we plot the isosurfaces of band decomposed charge density corresponding to CBM and VBM in Figs. 1(c) and 1(d), respectively. As expected, the distribution of VBM and CBM is spatially well separated: the former mainly originates from the nitrogen p_z states and the latter is attributed to the C=C antibonding π states, which is perfect for the separation of photogenerated electron–hole pairs. However, the band gap value of 2.45 eV is too large to utilize the major part of the solar spectrum, and it is imperative to regulate the band gap of this material.

Doping with foreign elements has been confirmed as an effective method for tuning the electronic band structure of semiconductor, due to the difference in the energy level of the dopant element compared with that of the host element.[34,35] We investigate the effect of doping with different nonmetal elements like boron, oxygen, phosphorus, and sulfur. We consider two possible positions for each kind of dopant, that is, the dopant substitutes nitrogen (denoted as X_N, X = B, O, P or S), and it replaces the carbon atom (referred as X_C). After relaxation, we find that X_N is energetically more favorable (see Table 1 for the lower formation energy) in comparison with X_C. We only focus on X_N-doped C_2N in the following discussions.

In Table 2, we list the lattice parameters and the related bond lengths of X_N in different cases. For all the dopants considered, the lattice constant changes within 1%, the change of the bond length of C–C and C–N could be ignored. While for P_N and S_N, the bond length of P (or S) and carbon is stretched up to 22%, and their formation energies are larger than 2.3 eV, indicating that P and S will not exist in high concentration under thermal equilibrium. Moreover, by looking at the band structures as presented in Fig. 2, we note that both oxygen and sulfur doping introduce isolated donor states below the CBM, which could act as the recombination center and hence decrease the efficiency of the catalyst. For B_N and P_N, the band gap is reduced to 2.01 eV and 2.08 eV, respectively, without creating any undesirable gap states in the forbidden region. The lowest formation energy (0.19 eV) of B_N suggests a good incorporation of boron in C_2N.

Table 1. The formation energy (E_f) in unit eV for different dopants in C_2N sheet.

Dopant	E_f	Dopant	E_f
B_N	0.19	B_C	2.18
O_N	0.70	O_C	6.64
P_N	2.36	P_C	6.51
S_N	2.39	S_C	8.44

Table 2. The lattice parameters, bond lengths of C_2N, and its doped cases.

Configurations	a/Å	d_{C-N}/Å	d_{C-C}/Å	$d_{Dopant-C}$/Å
Clean C_2N	8.33	1.34	1.43/1.47	–
B_N	8.40	1.34	1.45/1.45	1.42
O_N	8.30	1.35	1.41/1.43	1.37
P_N	8.41	1.35	1.43/1.45	1.73
S_N	8.39	1.35	1.42/1.43	1.71

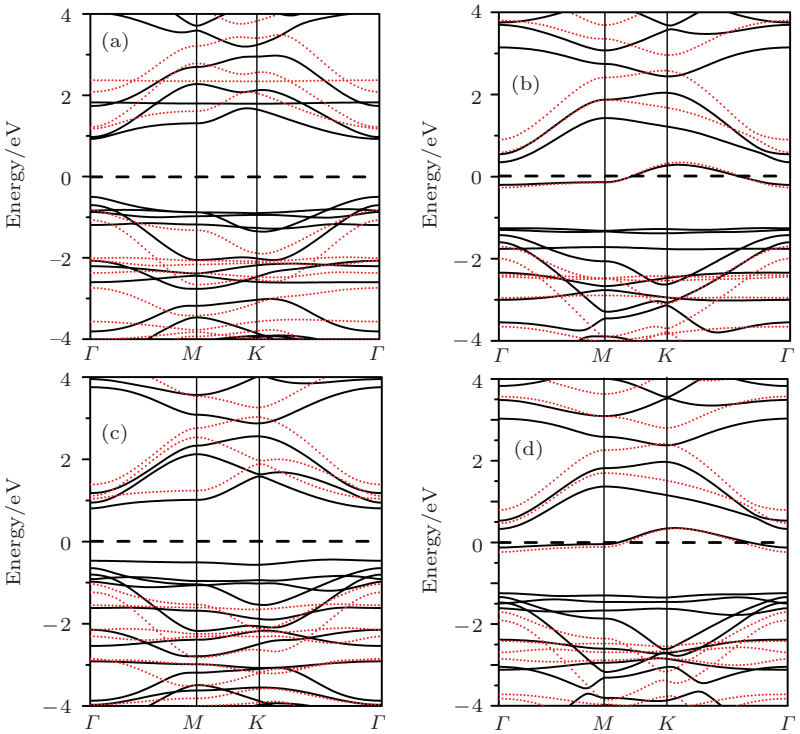


Fig. 2. (color online) (a)–(d) Band structures of B-, O-, P-, and S-doped C_2N calculated by PBE (black solid lines) and HSE06 (red dashed lines).

To see if the photocatalyst is high-efficiency visible light-sensitive, we have calculated the complex frequency-dependent dielectric function $\varepsilon(\omega) = \varepsilon_1(\omega) + i\varepsilon_2(\omega)$, where ε_1 and ε_2 represent the real and imaginary parts of the dielectric function, respectively. The absorption coefficient $\alpha(\omega)$ has been obtained from the relation[33]

$$\alpha(\omega) = \sqrt{2}\omega\left[\sqrt{\varepsilon_1(\omega)^2 + \varepsilon_2(\omega)^2} - \varepsilon_1(\omega)\right]^{1/2}. \quad (2)$$

The absorption spectra for the intrinsic single layer C_2N along with its boron and phosphorus substituted systems are shown in Fig. 3. Clearly, the undoped C_2N has a strong absorption peak around 450 nm–500 nm. However, for boron and phosphorus doped structures, the absorption curves are extended toward the whole visible light region, indicating the improved visible light activity.

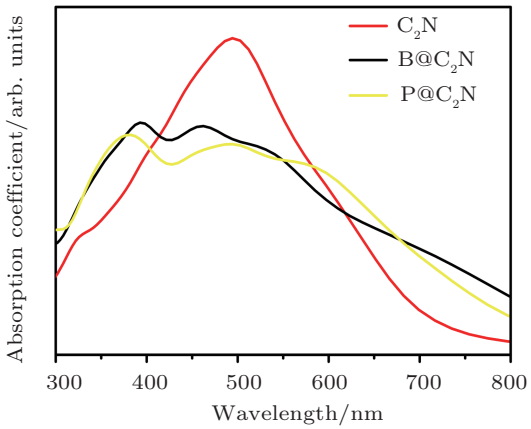


Fig. 3. (color online) Calculated optical absorption spectra of different C_2N systems considered.

The better visible light activity is a necessary condition for photocatalytic water splitting using solar light, it is not sufficient. To generate hydrogen and oxygen from water splitting, the band edges should be positioned appropriately with respect to the redox levels of water. The band edge alignments of monolayer C_2N, boron, and phosphorus doped C_2N are plotted in Fig. 4. The standard water reduction and oxidation potential levels are marked for reference. Note that different systems have different Fermi levels, while the vacuum levels on both sides of the system are equal. We align the energy levels according to the following procedure: for each system, we figure out its vacuum level, VBM and CBM positions, and then refer them to the vacuum level of the pure C_2N. For the single layer C_2N, the CBM and VBM are found to be located at -4.10 eV and -6.55 eV, respectively. The CBM is located at 0.30 eV above the water reduction level, whereas the VBM is found to be 0.88 eV below the water oxidation potentials. The photocatalytic performance of g-C_3N_4 is also included for comparison, it can be seen that C_2N is better with more suitable CBM positions. For the case of boron- and phosphorus-doped C_2N, the change in CBM is found to be negligible, while the VBM shift upward. These band alignments show that both the oxidation and reduction reactions of water are thermodynamically feasible in doped$-C_2N$, therefore, this novel 2D material can be expected to be a good photocatalyst for hydrogen generation under visible light. Nonmetallic doping in graphene and g-C_3N_4 has been experimentally achieved,[36–38] the synthesis of boron- or phosphorus-doped C_2N would be expectable.

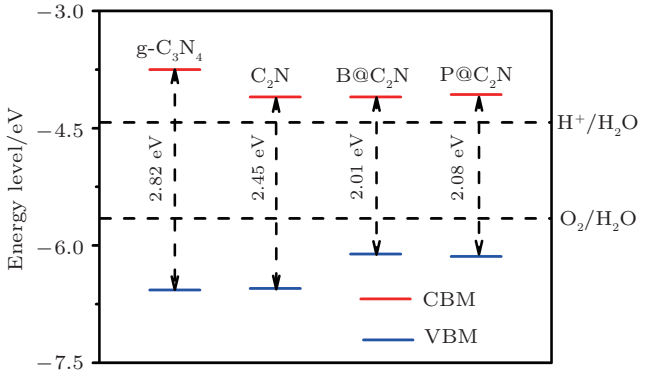


Fig. 4. (color online) Calculated VBM and CBM positions of g-C_3N_4, C_2N and along with the boron and phosphorus doped counterparts.

4. Conclusions

In summary, we have explored the possible photocatalytic activity of 2D graphitic carbon nitrides toward the water splitting under visible light. Single layer C_2N is a semiconductor with a direct band gap of 2.45 eV. The effect of doping with nonmetal elements, boron, phosphor, oxygen, and sulfur on the electronic band structure of C_2N has been investigated. Substitutional doping with boron and phosphorus in C_2N could improve the visible light absorption significantly by reducing the band gap to close 2 eV, and importantly, no defect states in the gap. For intrinsic and B- (or P-)doped C_2N, the positions of band edges with respect to water redox levels satisfy the thermodynamic criteria for overall water splitting. Note that the phosphorus doping has the higher formation energy, indicating that it will not exist in high concentration under thermal equilibrium. Experiments are called for to investigate this prediction.

References

[1] Lewis N S and Nocera D G 2006 *Proc. Natl. Acad. Sci.* **103** 15729
[2] Züttel A, Remhof A, Borgschulte A and Friedrichs O 2010 *Philosophical Transactions* **368** 3329
[3] Gregoirepadró C E 1998 *Energy and Fuels* **12** 337
[4] Dinga G P 1988 *Int. J. Hydrogen Energy* **14** 777
[5] Navarro Yerga R M 2009 *Chemsuschem* **2** 471
[6] Bard A J and Fox M A 1995 *Acc. Chem. Res.* **28** 141
[7] Fujishima A and Honda K 1972 *Nature* **238** 37
[8] Yamaguti K and Sato S 1985 *J. Chem. Soc. Faraday Trans.* **81** 1237
[9] Haruhiko K, Nobuo S, Hiroshi N, Hisayoshi K, Yoshiki S, and Yasunobu I 2007 *J. Phys. Chem. C* **111** 439
[10] Katz J E, Gingrich T R, Santori E A and Lewis N S 2008 *Energy Environ. Sci.* **2** 103
[11] Zhao Z G and Miyauchi M 2008 *Angewandte Chemie* **47** 7051

[12] Cui Z, Zeng D, Tang T, Liu J and Xie C 2010 *Journal of Hazardous Materials* **183** 211
[13] Maschmeyer T and Che M 2010 *Angewandte Chemie* **49** 1536
[14] Xiang Q, Yu J and Jaroniec M 2012 *Chem. Soc. Rev.* **41** 782
[15] Balzani V, Credi A and Venturi M 2008 *Chemsuschem* **1** 26
[16] Ran J, Zhang J, Yu J, Jaroniec M and Qiao S Z 2014 *Chem. Soc. Rev.* **43** 7787
[17] Molinari R, Marino T and Argurio P 2014 *Int. J. Hydrogen Energy* **39** 7247
[18] Wang X, Maeda K, Thomas A, Takanabe K, Xin G, Carlsson J M, Domen K and Antonietti M 2009 *Nat. Mater.* **8** 76
[19] Zhang J, Chen X, Takanabe K, Maeda K, Domen K, Epping J D, Fu X, Antonietti M and Wang X 2010 *Angewandte Chemie* **49** 441
[20] Zhang Y, Mori T, Li N and Ye J 2011 *Energy Environ. Sci.* **4** 4517
[21] Ma X, Lv Y, Xu J, Liu Y, Zhang R and Zhu Y 2012 *J. Phys. Chem. C* **116** 23485
[22] Zheng Y, Liu J, Liang J, Jaroniec M and Qiao S Z 2012 *Energy Environ. Sci.* **5** 6717
[23] Pan H, Zhang Y W, Shenoy V B and Gao H 2011 *Acs Catalysis* **1** 99
[24] Wang J, Guan Z, Huang J, Li Q and Yang J 2014 *J. Mater. Chem. A* **2** 7960
[25] Mahmood J 2015 *Nat. Commun.* **6** 6486
[26] Blöchl P E 1994 *Phys. Rev. B* **50** 17953
[27] Kresse G and Joubert D 1999 *Phys. Rev. B* **59** 1758
[28] Kresse G and Furthmüller J 1996 *Phys. Rev. B* **54** 11169
[29] Kresse G and Furthmüller J 1996 *Comput. Mater. Sci.* **6** 15
[30] Perdew J P, Burke K and Ernzerhof M 1996 *Phys. Rev. Lett.* **77** 3865
[31] Heyd J, Scuseria G E and Ernzerhof M 2003 *J. Chem. Phys.* **118** 8207
[32] Momma K and Izumi F 2001 *J. Appl. Crystallography* **41** 653
[33] Srinivasu K, Modak B, and Ghosh S K 2014 *Phys. Rev. Lett.* **118** 26479
[34] Modak B, Srinivasu K and Ghosh S K 2014 *Phys. Chem. Chem. Phys.* **16** 17116
[35] Modak B, Srinivasu K and Ghosh S K 2014 *Rsc Adv.* **4** 45703
[36] Liu G, Niu P, Sun C, Smith S C, Chen Z, Lu G Q and Cheng H M 2010 *J. Am. Chem. Soc.* **132** 11642
[37] Hu S, Ma L, You J, Li F, Fan Z, Wang F, Liu D and Gui J 2014 *Rsc Adv.* **4** 21657
[38] Choi C H, Park S H and Woo S I 2012 *ACS Nano* **6** 7091